



A novel anti-microtubule agent with carbazole and benzohydrazide structures suppresses tumor cell growth *in vivo*



Makoto Ohira^{a,1}, Yuka Iwasaki^{a,1}, Chika Tanaka^{a,1}, Michitaka Kuroki^{a,1}, Naoki Matsuo^a, Tatsuhiko Kitamura^a, Masaki Yukuhiro^a, Hiroyuki Morimoto^b, Nisha Pang^b, Bei Liu^b, Tohru Kiyono^c, Masahide Amemiya^d, Kozo Tanaka^e, Kazumasa Yoshida^a, Nozomi Sugimoto^a, Takashi Ohshima^{b,*}, Masatoshi Fujita^{a,**}

^a Department of Cellular Biochemistry, Graduate School of Pharmaceutical Sciences, Kyushu University, 3-1-1 Maidashi, Higashi-ku, Fukuoka 812-8582, Japan

^b Department of Green Pharmaceutical Chemistry, Graduate School of Pharmaceutical Sciences, Kyushu University, 3-1-1 Maidashi, Higashi-ku, Fukuoka 812-8582, Japan

^c Division of Carcinogenesis and Cancer Prevention, National Cancer Center Research Institute, 5-1-1 Tsukiji, Chuo-ku, Tokyo 104-0045, Japan

^d Institute of Microbial Chemistry (BIKAKEN), Numazu, 18-24 Miyamoto, Numazu-shi, Shizuoka 410-0301, Japan

^e Department of Molecular Oncology, Institute of Development, Aging and Cancer, Tohoku University, 4-1 Seiryomachi, Aoba-ku, Sendai, Miyagi 980-8575, Japan

ARTICLE INFO

Article history:

Received 13 February 2015

Received in revised form 28 April 2015

Accepted 30 April 2015

Available online 7 May 2015

Keywords:

Anti-mitotic agents
Anti-neoplastic agents
Centrosome
Microtubules
Mitotic spindle

ABSTRACT

Background: The mitotic spindles are among the most successful targets of anti-cancer chemotherapy, and they still hold promise as targets for novel drugs. The anti-mitotic drugs in current clinical use, including taxanes, epothilones, vinca alkaloids, and halichondrins, are all microtubule-targeting agents. Although these drugs are effective for cancer chemotherapy, they have some critical problems; e.g., neurotoxicity caused by damage to neuronal microtubules, as well as innate or acquired drug resistance. To overcome these problems, a great deal of effort has been expended on development of novel anti-mitotics.

Methods: We identified novel microtubule-targeting agents with carbazole and benzohydrazide structures: *N'*-(9-ethyl-9*H*-carbazol-3-yl)methylene]-2-methylbenzohydrazide (code number HND-007) and its related compounds. We investigated their activities against cancer cells using various methods including cell growth assay, immunofluorescence analysis, cell cycle analysis, tubulin polymerization assay, and tumor inhibition assay in nude mice.

Results: HND-007 inhibits tubulin polymerization *in vitro* and blocks microtubule formation and centrosome separation in cancer cells. Consequently, it suppresses the growth of various cancer cell lines, with IC_{50} values in the range 1.3–4.6 μ M. In addition, HND-007 can inhibit the growth of taxane-resistant cancer cells that overexpress P-glycoprotein. Finally, HND-007 can inhibit HeLa cell tumor growth in nude mice.

Conclusions and general significance: Taken together, these findings suggest that HND-007 is a promising lead compound for development of novel anti-mitotic, anti-microtubule chemotherapeutic agents.

© 2015 Elsevier B.V. All rights reserved.

1. Introduction

The mitotic spindles are among the most successful targets of anti-cancer chemotherapy, and they still hold promise as targets of novel drugs [1–4]. In mammalian somatic cells, the fundamental machinery of the mitotic spindles comprises the spindle microtubules, composed

of polymerized α -tubulin and β -tubulin heterodimers, and centrosomes, which contain two centrioles and are duplicated during the interphase. Spindle microtubule nucleation is initiated from centrosomes, and the polymerization and depolymerization dynamics must be tightly spatiotemporally regulated to ensure proper mitotic progression. In addition, many MAPs (microtubule-associated proteins) are also required for mitosis, including the dynein and kinesin motor proteins, as well as many microtubule-regulatory proteins such as ch-TOG. Under the control of mitotic kinases such as Cdk1, Aurora kinases, and Polo-like kinases (Plks), these factors function in a highly coordinated manner to ensure proper progression of mitosis.

The anti-mitotic drugs in current clinical use are taxanes, epothilones, vinca alkaloids, and halichondrins, all of which are microtubule-targeting agents that bind to tubulin molecules [2,4]. The former two classes of compounds inhibit depolymerization of microtubules (microtubule

* Correspondence to: T. Ohshima, Department of Green Pharmaceutical Chemistry, Graduate School of Pharmaceutical Sciences, Kyushu University, 3-1-1 Maidashi, Higashi-ku, Fukuoka 812-8582, Japan. Tel./fax: +81 92 642 6650.

** Correspondence to: M. Fujita, Department of Cellular Biochemistry, Graduate School of Pharmaceutical Sciences, Kyushu University, 3-1-1 Maidashi, Higashi-ku, Fukuoka 812-8582, Japan. Tel./fax: +81 92 642 6635.

E-mail addresses: ohshima@phar.kyushu-u.ac.jp (T. Ohshima),

mfujita@phar.kyushu-u.ac.jp (M. Fujita).

¹ These authors equally contributed to this work.

stabilizers), whereas the latter two prevent polymerization (microtubule destabilizers); both lead to mitotic arrest, cell growth arrest, and eventual cell death. Cancer cells are more susceptible than non-transformed cells to microtubule-targeting agents, although our understanding of the underlying molecular mechanisms is limited [5–7]. In addition, the molecular basis of the tissue specificities of microtubule-targeting agents also remains to be clarified. It was recently suggested that some microtubule-targeting agents disrupt the tumor vasculature [8].

Although these clinically used drugs are effective for cancer chemotherapy, there are some critical problems to be solved. For example, because microtubules play important roles in non-dividing cells like neuronal cells, these drugs inevitably damage such cells, resulting in adverse effects such as peripheral neuropathy. Another issue is innate or acquired resistance to microtubule-targeting agents. The known mechanisms that confer resistance to the microtubule-targeting drugs include overexpression of a class of ATP-dependent membrane transporter proteins represented by MDR1, overexpression of specific isoforms of tubulin such as β III-tubulin, certain mutations in tubulin, and overexpression of certain MAPs [2,4,9]. To overcome these problems, a great deal of effort has been devoted to development of novel anti-mitotics that target non-microtubule mitotic proteins such as Aurora kinases, Plks, Eg5, and CENP-E [3,10–16]. Unfortunately, thus far, the clinical efficacy of these novel anti-mitotics has been limited [3].

Novel microtubule-targeting agents would also be valuable [2–4,17,18]. Among the microtubule-targeting agents in current clinical use, vinca alkaloids and halichondrins bind to a specific site on tubulin termed the “vinca site”, whereas taxanes and epothilones bind to another site termed the “taxane site” [4]. Another site recognized by microtubule-targeting agents is the “colchicine site” [4]; however, so far, no drug that binds to the colchicine site has been deployed for cancer chemotherapy. Nevertheless, ongoing efforts are still being devoted to development of such colchicine site-binding drugs, especially as vascular disrupting agents [4,8,18]. Recently, the laulimalide/peloruside-binding site on tubulin molecules has been also identified, although a short supply of the natural products has prevented clinical trials of these compounds [19].

In this report, we describe novel microtubule-targeting agents with carbazole and benzohydrazide structures that were identified during the course of screening for inhibitors of Cdt1-geminin binding (for details, see Results and discussion). Among them, *N*'-[(9-ethyl-9*H*-carbazol-3-yl)methylene]-2-methylbenzohydrazide (code number HND-007) can suppress tumor cell growth *in vitro* and *in vivo*.

2. Materials and methods

2.1. Cell culture

HeLa (cervical carcinoma), H1299 (non-small cell lung carcinoma), HCT116 (colon carcinoma), T98G (glioblastoma), and HFF2/T (normal human fibroblasts immortalized by telomerase) cells were grown in Dulbecco's modified Eagle's medium supplemented with 8% fetal calf serum (FCS). PC-14 and PC-14/TXT cells were kindly provided by Dr. Fumiaki Koizumi (National Cancer Center, Japan).

2.2. Drugs

Drugs used in this study were as follows: nocodazole (Sigma-Aldrich, M1404), paclitaxel (BML, T104-0005), and hydroxyurea (Sigma-Aldrich, H8627).

2.3. Growth inhibition assay

Cells were plated in 96-well plates at 5×10^3 cells/well, and the indicated compounds dissolved in DMSO were added 24 h later. DMSO (vehicle) was added to control cells at a final concentration of 1%. After treatment for 48 h, MTS/PMS solution (CellTiter Aqueous Non-

Radioactive Cell Proliferation Assay, #G5430, Promega) was added, cells were further incubated for 1 h, and OD₄₉₀ was measured to determine cell number. The percent inhibition was determined for each drug concentration, and the IC₅₀ value for cell growth was calculated from the linear portion of the dose-response curve using regression analysis.

2.4. Tumor studies in nude mice

The protocols for animal experiments were approved by the Kyushu University Animal Care and Use Committee (permit number: A23-067 and A25-022). Four-week-old female BALB/c *nu/nu* nude mice were obtained from Kyudo Co., Ltd. Mice were inoculated by subcutaneous injection on their backs with 1×10^6 HeLa cells mixed with Matrigel (50 μ L of cell suspension + 50 μ L of Matrigel, 356234, BD Biosciences). The size of the xenografted tumor was measured using digital calipers, and volume was calculated based on the following formula: tumor volume (mm³) = length \times (width)² \times $\pi/6$. Body weight and tumor size were measured three times per week. Once the tumor reached ~ 100 mm³, mice were randomly divided into two groups, one receiving the control vehicle mixture detailed below and the other receiving vehicle plus HND-007 (50 mg/kg). Drug was administered intraperitoneally once daily for 3 days. Vehicle mixture consisted of 20% DMSO, 20% Cremophor (polyoxyethylene castor oil), 20% ethanol, and 40% saline.

2.5. Tubulin polymerization assay

Tubulin polymerization assays were performed using the HTS-tubulin Polymerization Kit (Cytoskeleton, BK004P). The reaction was conducted in the presence of 10% glycerol and 3.35 mg/ml tubulin. Drugs were dissolved in DMSO and added to the reaction mixtures; the final concentration of DMSO was 2%. Tubulin polymerization was monitored by measuring OD₃₄₀ at 37 °C.

2.6. Immunoblot analysis and antibodies

Immunoblot analysis was performed as described previously [20]. Antibodies used were as follows: phospho-Histone H3 Ser10 (#9706, Cell Signaling Technology, 1:1000 dilution); Cdc2-phosphorylated vimentin Ser55 (D076-3, MBL, 1:20 dilution); phospho-cyclinB1 Ser133 (#4133S, Cell Signaling, 1:1000 dilution); PARP1 (#9542, Cell Signaling Technology, 1:1000 dilution); α -tubulin (ab15246, Abcam, 1:100 dilution for immunofluorescence); γ -tubulin (T6557, Sigma-Aldrich, 1:2000 dilution for immunofluorescence); centrin1 (ab11257, Abcam, 1:200 dilution for immunofluorescence); CENP-B (kindly provided by Dr. Hiroshi Masumoto, Kazusa DNA Research Institute, 1:200 dilution for immunofluorescence). For secondary antibodies, HRP-rabbit anti-mouse IgG (H + L) (61-6520, Invitrogen, 1:1000 dilution) or HRP-goat anti-rabbit IgG (H + L) (65-6120, Invitrogen, 1:1000 dilution) were used.

2.7. Immunofluorescence analysis

Cells were fixed with 3.7% formaldehyde in PBS for 10 min at RT (Room Temperature) and further treated with 100% ice-cold MeOH for 15 min. The cells were then permeabilized with 0.1% Triton X-100, incubated with primary antibodies (diluted with PBS containing 10% FCS) for 1 h at RT, and washed three times with PBS. For centrin1 staining, cells were treated with ice-cold MeOH for 5 min and then incubated with anti-centrin1 antibody overnight at RT. Cells were then incubated with secondary antibodies for 1 h at RT and finally counterstained with 4,6-diamidino-2-phenylindole (DAPI). The samples were mounted in Vectashield (Vector Laboratories) and analyzed on a Zeiss LSM700 microscope. Secondary antibodies used were CF594-conjugated goat anti-mouse IgG (H + L) (20111, Biotium, 1:100 dilution) and CF488-conjugated goat anti-rabbit IgG (H + L) (20019, Biotium, 1:100 dilution).

For analysis of cold-stable microtubules [21], cells were first treated with the indicated compounds or control DMSO for 6 h, then placed on ice for 10 min, and finally fixed as above.

2.8. Cell-cycle analysis

Cells were treated with the compounds for 24 h, and then suspended in phosphate-buffered saline (PBS) containing 0.1% Triton X-100 and RNase (10 $\mu\text{g}/\text{mL}$). After staining with propidium iodide (40 $\mu\text{g}/\text{mL}$), cell-cycle distribution was examined using a FACSCalibur flow cytometer (BD Bioscience).

2.9. Statistical analysis

Unless otherwise stated, statistical analyses were performed using a two-tailed Student's *t*-test. *p* values of <0.05 were considered statistically significant.

3. Results and discussion

3.1. Identification of *N'*-[(9-ethyl-9*H*-carbazol-3-yl)methylene]-2-iodobenzohydrazide (code number NP-10) and related compounds (HND-007 and NP-14) as novel potent anti-neoplastic agents with carbazole and benzohydrazide structures

We sought to identify novel inhibitors of Cdt1-geminin binding as possible anti-neoplastic agents [22]. To this end, we screened ~20,000 compounds, including commercially available chemical libraries and in-house chemicals, according to a previously published method using purified recombinant Cdt1 and geminin proteins [22]. We identified several compounds that yielded low signals in the assay potentially resulting from inhibition of *in vitro* Cdt1-geminin binding (data not shown). Among these compounds was one from a commercially available chemical library (ChemBridge), *N'*-[(9-ethyl-9*H*-carbazol-3-yl)methylene]-2-iodobenzohydrazide (lot number 5194537). We examined the effect of lot 5194537 on the cell-cycle profiles of cervical cancer-derived HeLa cells and HFF2/T cells, normal human fibroblasts immortalized by telomerase. When cells were treated for 24 h at a concentration of 10 μM , flow-cytometric analysis revealed obvious G2/M-phase arrest in HeLa cells but not HFF2/T cells (data obtained with the original 5194537 are not shown, but more detailed analyses with the in-house-synthesized compound are shown below). Although re-replication, a phenotype observed when the function of geminin is sequestered [23], was not induced by the drug treatment, the apparently cancer-selective cell-cycle arrest was of interest. Hence, we synthesized the compound (code number NP-10) for further detailed studies (Fig. 1). As expected, like the original lot 5194537, NP-10 had cancer-selective G2/M arrest activity (see below). However, NP-10 did not inhibit Cdt1-geminin binding (data not shown). It is possible that the original lot 5194537 contained some contaminating chemicals that affect Cdt1-geminin binding *in vitro*. Unfortunately, because the residual quantity of 5194537 was not sufficient for further analysis, we could not investigate this possibility.

The chemical library also included a closely related compound, *N'*-[(9-ethyl-9*H*-carbazol-3-yl)methylene]-2-methylbenzohydrazide (lot number 5194550), which has a methyl moiety at the *ortho* position of the benzene ring instead of the *ortho*-iodo moiety in NP-10. We found that it also induced G2/M arrest in HeLa cells (data from the original 5194550 not shown), so we synthesized and analyzed it (code number HND-007; Fig. 1). In addition, we also synthesized *N'*-[(9-ethyl-9*H*-carbazol-3-yl)methylene]-4-iodobenzohydrazide (code number NP-14), which has an iodo moiety at the *para* position of the benzene ring instead of the *ortho* position as in NP-10 (Fig. 1). This compound also induced a G2/M arrest phenotype in HeLa cells (see below).

3.2. NP-10, HND-007, and NP-14 all inhibit mitotic progression in cancer-derived cells, but the execution points may differ between NP-10 and HND-007/NP-14

We first estimated the IC_{50} (50% inhibition concentration) values for growth of four human cancer cell lines (HeLa, H1299, HCT116, and T98G) and HFF2/T cells (Table 1). NP-10 inhibited the growth of the cancer cells with estimated IC_{50} values of 3.7–11 μM . On the other hand, higher concentrations were required to inhibit the growth of HFF2/T cells, with an estimated IC_{50} value of 21 μM . In this study, we calculated the ratio between the IC_{50} for HFF2/T and the IC_{50} for HeLa as one potential index (cancer cell selectivity index) indicating the cancer selectivity of growth-inhibitory compounds. For NP-10, the ratio was estimated to be ~5.6-fold (Table 1). HND-007 inhibited the growth of the cancer cells more effectively than NP-10, with IC_{50} values of 1.3–4.6 μM . However, the cancer cell selectivity index (~3.4) was lower than that of NP-10. NP-14 was also a potent inhibitor of cancer cell growth, with IC_{50} values of 1.3–4.4 μM , comparable to those of HND-007, and its selectivity (~2.5) was also similar to that of HND-007. We also examined the abilities of two well-known anti-mitotic agents, vincristine and paclitaxel, to inhibit HeLa and HFF2/T growth

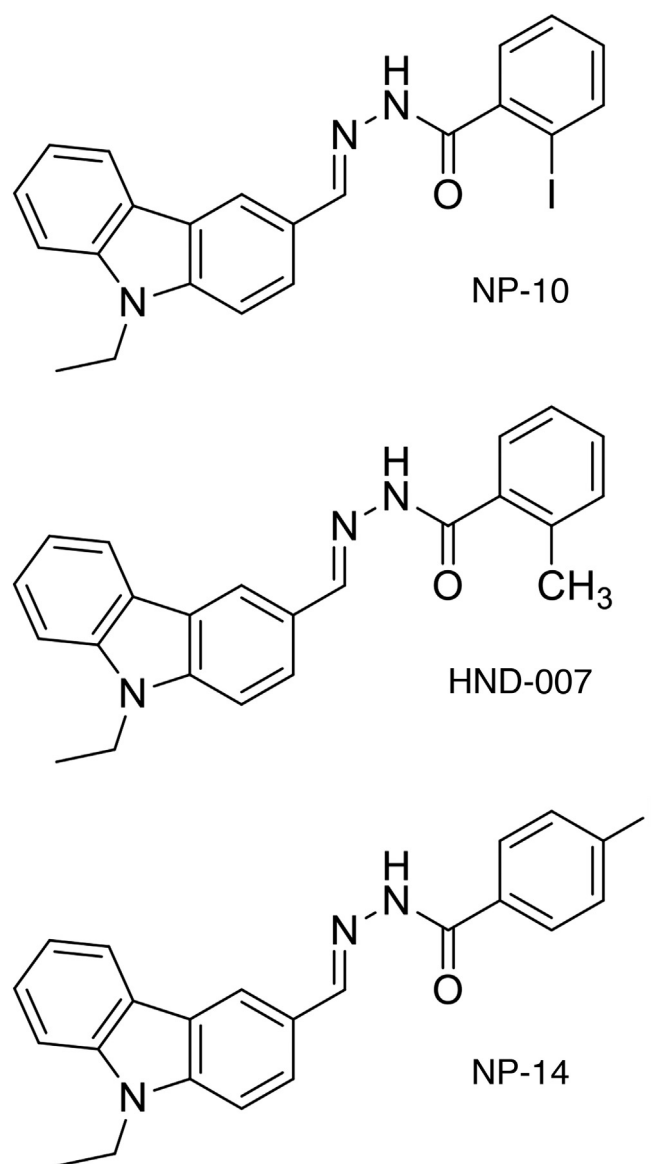


Fig. 1. Chemical structures of NP-10, HND-007, and NP-14.

Table 1
Inhibition of *in vitro* cell growth by the compounds used in this study.

Compound	IC ₅₀ (mean ± S.D.) [‡]					Selectivity index [§]
	HeLa [†]	T98G	H1299	HCT116	HFF2/T	
NP-10	3.72 ± 0.63	5.28 ± 0.88	10.9 ± 0.86	5.94 ± 0.35	20.7 ± 4.36	5.56
HND-007	1.27 ± 0.18	2.25 ± 0.04	4.57 ± 1.26	2.22 ± 0.19	4.33 ± 0.64	3.40
NP-14	1.29 ± 0.18	2.78 ± 0.92	4.42 ± 1.09	1.60 ± 0.32	3.18 ± 0.39	2.47
Paclitaxel	7.74 ± 0.76	N.D.	N.D.	N.D.	13.5 ± 3.04	1.74
Vincristine	7.21 ± 0.52	N.D.	N.D.	N.D.	10.4 ± 1.39	1.45

[†] Cell lines used; HeLa: cervical carcinoma, T98G: glioblastoma, H1299: non-small cell lung carcinoma, HCT116: colon carcinoma, and HFF2/T: normal human fibroblasts immortalized by telomerase.

[‡] The units of IC₅₀ for NP-10, HND007, and NP-14 are μM, and the units for paclitaxel and vincristine are nM.

[§] Selectivity index means the ratio between the IC₅₀ for HFF2/T cells and the IC₅₀ for HeLa cells. n = 3–8, except for in the case of HND-007-treated T98G cells, for which n = 2.

under our assay conditions (Table 1). Vincristine inhibits tubulin polymerization, whereas paclitaxel inhibits tubulin depolymerization. The IC₅₀ values of vincristine for HeLa cells and HFF2/T cells were ~7.2 nM and ~10 nM, respectively, with a selectivity index of ~1.5. The IC₅₀ values of paclitaxel for HeLa cells and HFF2/T cells were ~7.7 nM and ~14 nM, with a selectivity index of ~1.7. Thus, the potencies of these clinically used compounds to inhibit cancer cell growth *in vitro* was higher than those of HND-007 and NP-14, whereas their cancer cell selectivities were comparable to those of the novel compounds.

Among the compounds tested here, NP-10 might have favorable selectivity for inhibition of cancer cell growth *in vitro*.

We next used flow-cytometric analysis to investigate whether the growth-inhibitory effects of the novel compounds was the result of cell-cycle arrest at specific phase(s). At the appropriate concentrations (10 μM for NP-10, 3 μM for HND-007, and 1 μM for NP-14), the compounds selectively induced G2/M arrest in HeLa cells, but not HFF2/T cells (Fig. 2), although HFF2/T cells were also arrested at G2/M phase when treated with the compounds at higher concentrations

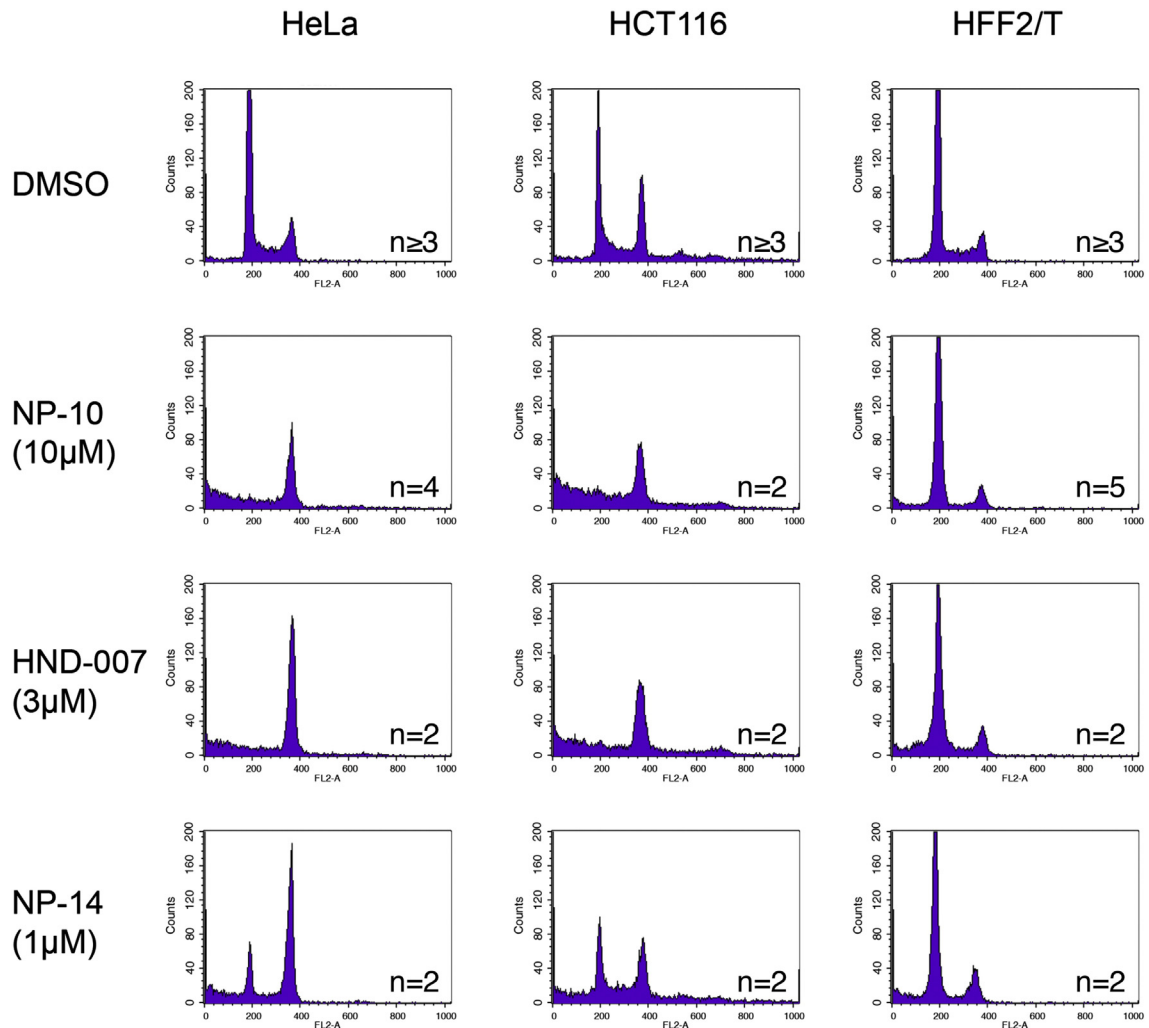


Fig. 2. The novel compounds induce G2/M arrest selectively in cancer-derived cell lines. HeLa, HCT116, and HFF2/T cells were treated with vehicle (DMSO) or the novel compounds at the indicated concentrations for 24 h. After staining with propidium iodide, cell-cycle distribution was analyzed by flow cytometry. Insets show the number of independent experiments.

(data not shown). Appearance of a sub-G1 population was also observed in drug-treated HeLa cells, suggesting induction of apoptosis. This idea was further supported by another assay (see below). Furthermore, these compounds induced similar G2/M arrest in other cancer-derived cells (Fig. 2). These results demonstrate that the novel compounds all induce G2 and/or mitotic arrest, leading to inhibition of cell growth.

Next, we asked whether the drug-treated cells are arrested at G2 or M phases. To address this issue, we first examined the levels of phospho-histone H3 Ser-10, a well-known mitotic marker [24]. The

levels increased comparably to those in cells treated with nocodazole, a well-known inhibitor of tubulin polymerization (Fig. 3a), indicating that all of the compounds prevent mitotic progression. We also examined the status of PARP protein. In agreement with the flow-cytometric analysis described above, a low-molecular weight, caspase-cleaved form of PARP, an apoptotic marker [25,26], was detected in the drug-treated cells (Fig. 3b).

We then examined in more detail the status of the mitotic arrest induced by these compounds by immunostaining of HeLa cells with anti- γ -tubulin and anti- α -tubulin antibodies (and DAPI for DNA

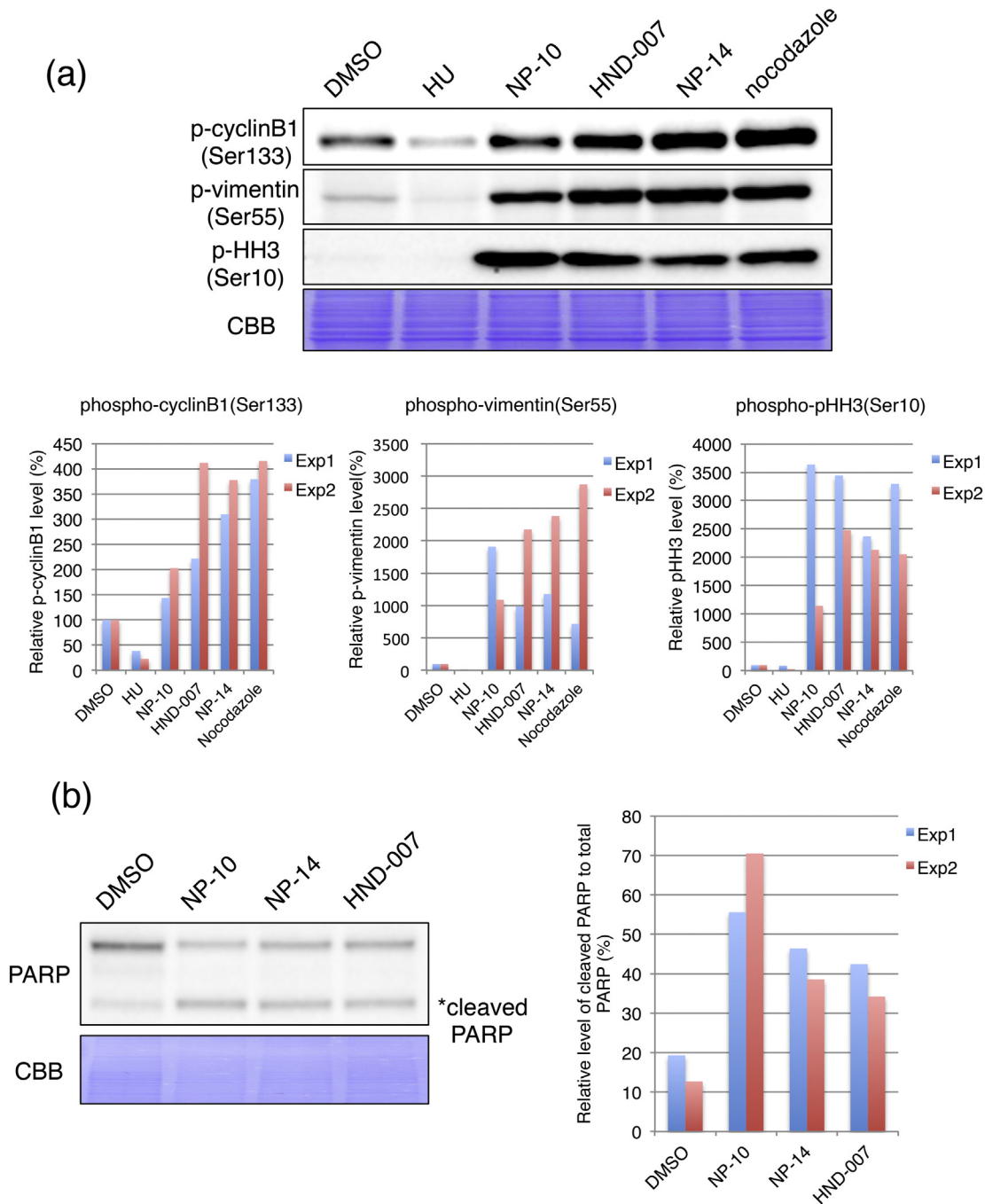


Fig. 3. Levels of mitotic phosphorylations and cleaved PARP are elevated in drug-treated cells. (a) HeLa cells treated with DMSO, the indicated compounds (10 μ M), hydroxyurea (HU which arrests cells in S phase; 2.5 mM), or nocodazole (1 μ M) for 24 h were subjected to immunoblotting with the indicated antibodies. Phospho-histone H3 (Ser-10) is a target of Aurora B Kinase; phospho-cyclin B1 (Ser-133) is a target of Plk1 kinase; and phospho-vimentin (Ser-55) is a target of Cdk1 kinase. The signal intensities of the bands were quantified and normalized to the signals for CBB bands. The data from two independent experiments are shown with the indicated protein levels in control DMSO-treated cells set at 100. (b) HeLa cells treated with the indicated compounds for 24 h were subjected to immunoblotting with anti-PARP antibody to detect the cleaved form of PARP, a marker of apoptosis. The signal intensities of non-cleaved PARP and the cleaved PARP were quantified, and the ratio of the cleaved PARP to total PARP was calculated. The data from two independent experiments are shown.

staining). γ -Tubulin is a component of centrosomes, whereas α -tubulin is a main component of microtubules. In control DMSO-treated cells, normal mitotic progression was observed (as a representative image, a metaphase cell is shown in Fig. 4a). By contrast, upon NP-10 treatment, most cells arrested between prophase and prometaphase, with condensed but not arranged chromosomes. In addition, the cells contained abnormal, often multiple (>3), spindles or asters with shortened microtubules (Fig. 4a). We counted the number of prominent γ -tubulin-positive foci, representing centrosomes or spindle poles in mitotic cells, which were identified by the presence of condensed chromosomes in DAPI staining. In control DMSO-treated HeLa cells, most cells (~90%) contained the normal two centrosomes, and the residual minor populations contained abnormal multiple (>3) centrosomes or spindle-like asters (Fig. 4b). By contrast, upon NP-10 treatment, the number of cells with multiple asters increased significantly, reaching ~50% of all mitotic cells. We carried out two additional experiments to further understand the mitotic abnormalities induced by NP-10. First, we analyzed cold-stable microtubules [21] in NP-10-treated HeLa cells

to know whether the shortened microtubules form end-on-attachment with kinetochores. As shown in Supplementary Fig. S1a, whereas spindle microtubules remained detectable after cold treatment by immunostaining with anti- α -tubulin antibody in control DMSO-treated cells, they collapsed in cells treated with low-dose nocodazole or NP-10, suggesting that microtubules cannot stably bind to kinetochore in NP-10-treated cells. Second, we counted the number of centrosomes in mitotic cells by immunostaining with anti-centrin1 antibody. Centrin1 is a component of centrosomes. In control DMSO-treated HeLa cells, most cell (~95%) contained two centrosomes each with two centrioles (*i.e.* total 4 centrioles per single mitotic cell), as expected (Supplementary Fig. S1b and c). Even in NP-10-treated multipolar HeLa cells with multiple prominent γ -tubulin-positive foci, most cells similarly contained two centrosomes each with two centrioles (Supplementary Fig. S1b and c), suggesting that NP-10 may induce spindle multipolarity without centrosome overduplication or cytokinesis failure [27].

On the other hand, the phenotypes of NP-14- or HND-007-treated cells differed from those with NP-10. Most cells arrested between

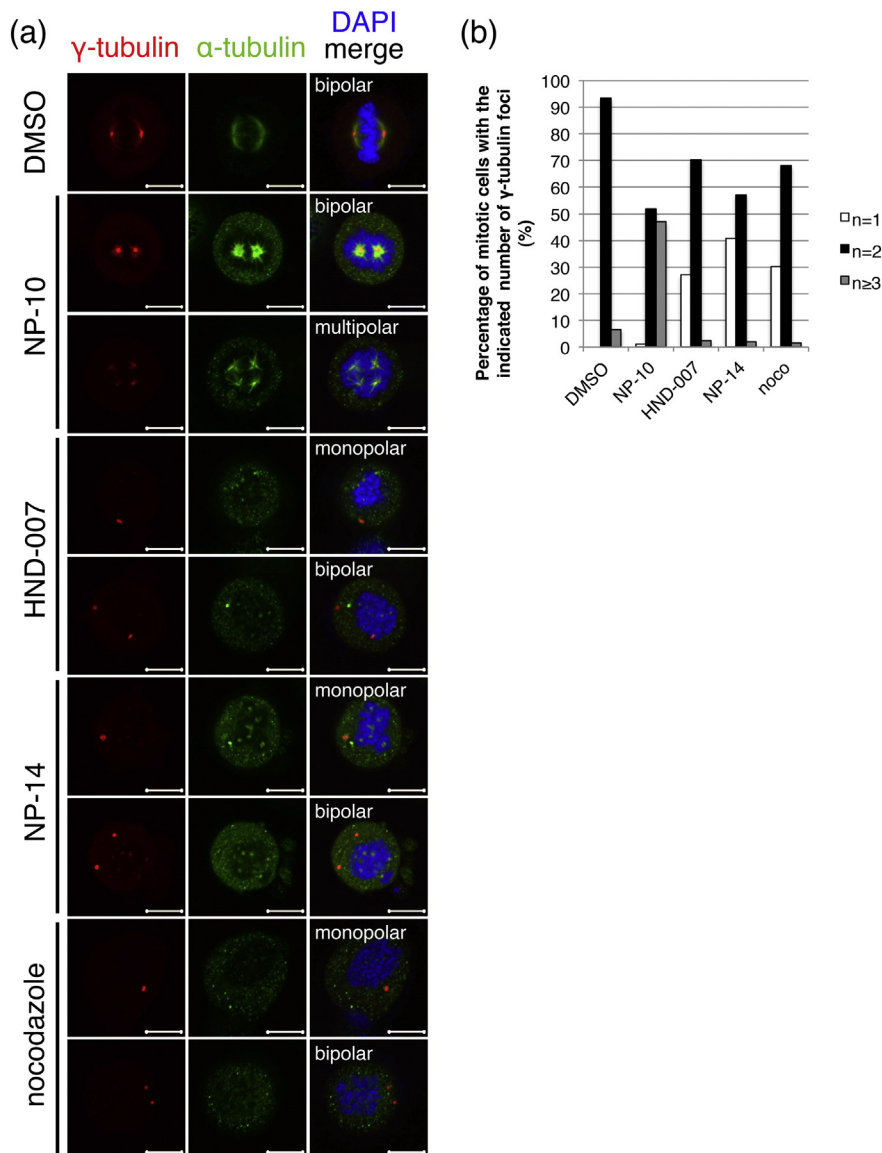


Fig. 4. NP-10, HND-007, and NP-14 induce aberrant mitotic spindles. (a) HeLa cells treated with the indicated compounds at 10 μ M for 6 h were subjected to immunofluorescence analysis with anti- α -tubulin antibody (green), anti- γ -tubulin antibody (red), and DAPI (blue). Representative images of aberrant spindles induced by each compound are shown. Scale bars, 10 μ m. (b) Percentages of mitotic cells, classified by number of prominent γ -tubulin foci, are shown for each compound. HeLa cells were treated as in (a), and the number of prominent γ -tubulin foci was counted. At least 100 randomly selected cells were subjected to the analysis. Nocodazole was used as a control inhibitor of tubulin polymerization. The number of prominent γ -tubulin foci reflects that of spindle poles: n = 1, monopolar; n = 2, bipolar; n \geq 3, multipolar. Essentially the same results were obtained in two independent experiments.

prophase and prometaphase, with condensed but not arranged chromosomes. However, in contrast to NP-10-treated cells, they often contained monomeric γ -tubulin-positive foci, probably representing non-separated centrosomes, with no visible microtubule formation (Fig. 4a). We counted the number of prominent γ -tubulin-positive foci, as above. In both NP-14- and HND-007-treated cells, the number of cells with monomeric centrosomes significantly increased (Fig. 4b). Overall, these phenotypes of NP-14- or HND-007-treated cells were very similar to those observed in nocodazole-treated cells (Fig. 4a and b).

Taken together, these findings indicate that the novel and structurally closely related compounds NP-10, NP14, and HND-007 hamper normal spindle formation, thereby inhibiting mitotic progression and inducing growth arrest and eventual cell death. However, NP-10 and HND-007/NP-14 may interfere with spindle formation in different ways. Because NP-10 and HND-007/NP-14 are structurally different only in the substituents of the benzene ring, it is surprising that such minor differences affect their target specificities. These findings regarding the structure–function relationship of these compounds will help to further optimize these compounds and increase their anti-tumor activities.

3.3. NP-10, HND-007, and NP-14 all inhibit cell growth of a taxane-resistant cancer cell line overexpressing P-glycoprotein

In clinical treatment with currently used anti-microtubule agents, one crucial problem to be solved is innate and acquired drug resistance [2,4]. Therefore, we examined whether our compounds can suppress the growth of taxane-resistant cancer cells. Accordingly, we tested the effect of our compounds on lung cancer-derived PC-14 cells and a paclitaxel-resistant derivative, PC-14/TXT, which overexpresses P-glycoprotein [28]. As expected, PC-14/TXT cells exhibited paclitaxel resistance in our assay, with a ~12-fold increase in the IC₅₀ value (Table 2). PC-14/TXT cells were also ~8.1-fold more resistant to vincristine. NP-10, NP-14, and HND-007 all inhibited cell growth of both PC-14 and PC-14/TXT at comparable concentrations, with IC₅₀ values of 7.6–10 μ M for NP10, 2.6–3.2 μ M for HND007, and 2.4–3.2 μ M for NP-14. Therefore, novel compounds could be effective for treatment of MDR-overexpressing, taxane- and/or vinca alkaloid-resistant tumors. However, it remains unclear whether the compounds can overcome taxane-resistance conferred by other mechanisms such as β -tubulin mutations [29].

3.4. NP-14 and HND-007, but not NP-10, inhibit tubulin polymerization *in vitro*

As described above, the phenotypes of NP-14- and HND-007-treated cells are similar to those of cells treated with nocodazole, a tubulin polymerization inhibitor. Hence, we examined whether the novel compounds could inhibit *in vitro* tubulin polymerization. For comparison, paclitaxel and nocodazole were also included in the assay. As shown

Table 2
Inhibition of *in vitro* growth of taxane-resistant cancer cells by the compounds used in this study.

Compound	IC ₅₀ (mean \pm S.D.) [‡]	
	PC-14 [†]	PC-14/TXT
NP-10	7.59 \pm 0.57	10.0 \pm 0.16
HND-007	2.62 \pm 0.11	3.19 \pm 0.34
NP-14	2.43 \pm 0.22	3.15 \pm 0.21
Paclitaxel	6.38 \pm 0.11	75.2 \pm 3.08
Vincristine	9.78 \pm 1.58	79.4 \pm 9.66

[†] Cell lines used; PC-14 (lung adenocarcinoma) and PC-14/TXT (taxane-resistant derivative of PC-14).

[‡] The units of IC₅₀ for NP-10, HND007, and NP-14 are μ M, and the units for paclitaxel and vincristine are nM. n = 3–8.

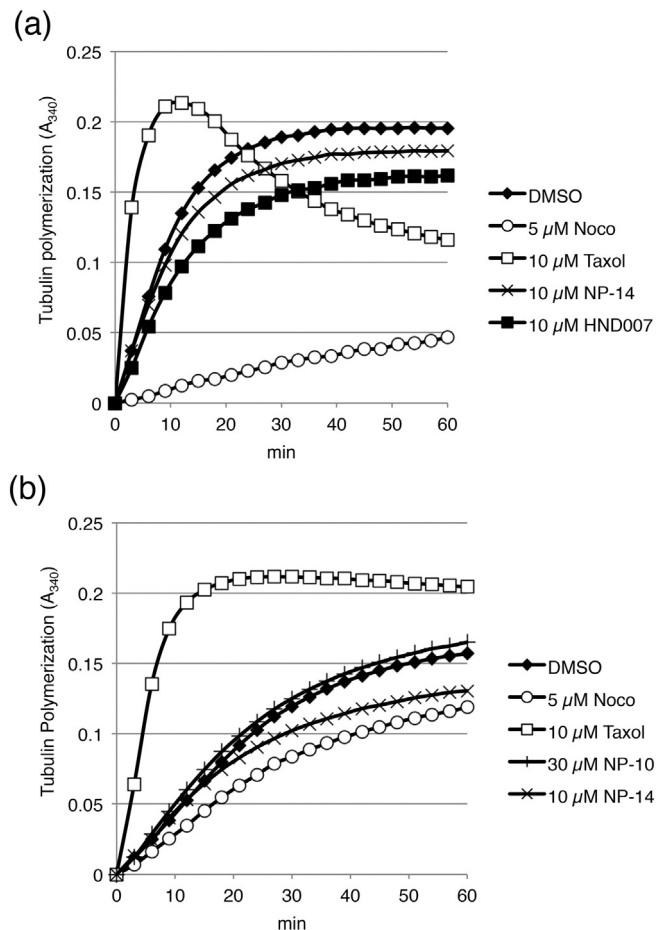


Fig. 5. HND-007 and NP-14, but not NP-10, partially inhibits tubulin polymerization *in vitro*. (a, b) Purified porcine brain tubulin was incubated in the presence of the indicated compounds at the indicated concentrations, and polymerization was monitored as described in Materials and methods. DMSO was used as a control vehicle. (a) and (b) were derived from two different experiments. See also Supplementary Fig. S2.

in Fig. 5a and Supplementary Fig. S2, NP-14 and HND-007 inhibited tubulin polymerization *in vitro* although to a lesser extent than nocodazole. Thus, the phenotypes observed following drug treatment may be at least partly attributable to inhibitory activity of these compounds on tubulin polymerization.

On the other hand, NP-10 did not inhibit *in vitro* tubulin polymerization at all (Fig. 5b and Supplementary Fig. S2). This seems consistent with the fact that microtubule formation is only partially inhibited in NP-10-treated cells, as shown above (Fig. 4a). Here, we further examined the possibility that NP-10 might affect some mitotic kinases and/or mitotic kinesins. For mitotic kinases, we examined the levels of phosphorylated forms of histone H3 Ser-10, cyclin B1 Ser-133, and vimentin Ser-55, which are phosphorylation targets of Aurora B, Plk1, and Cdk1, respectively [24,30,31]. However, all of the phosphorylated protein levels were maintained at high levels, comparable to those in nocodazole-treated cells, suggesting that the activities of these kinases were not impaired by the novel compounds (Fig. 3a). For the mitotic kinesins, we prepared the recombinant motor domain proteins (MDs) of CENP-E, Eg5, and KIFC1, and then investigated the effect of our compounds on the microtubule-dependent ATPase activity of the kinesin MDs. We were especially interested in the possibility that the novel compounds could affect Eg5 ATPase activity, because several compounds with carbazole structure inhibit the ATPase activity of Eg5 [11,12]. Moreover, KIFC1 inhibition may lead to multipolar spindles in certain cancer cells but not in non-transformed cells [32]. However, we did not observe any inhibitory effects on these enzymes (data not shown). At this time point, the reason(s) for the cancer cell selectivity of NP-10 remains unclear.

However, there are several possibilities that are not mutually exclusive. One is that the efficacy of intake and/or excretion of the compound might be different between HeLa and HFF2/T cells, for example by different expression of the related molecule(s) such as transporter(s). More intriguing possibility is that the compounds would interfere with molecule(s) involved in proper progression of mitosis and cancer cells more deeply depend on such molecule(s) for completion of mitotic progression. For example, Leber et al. identified multiple proteins required for centrosome clustering in cancer cells [33]. To further characterize the cancer cell-specific induction of multipolar spindles, we are currently trying to identify the molecular target(s) of NP-10.

3.5. HND-007 inhibits HeLa cell tumor formation in nude mice

Finally, we examined *in vivo* anti-tumor activities of these three compounds, using a HeLa cell xenograft model in nude mice. First, we determined the maximum tolerable doses for BALB/c mice with once daily intra-peritoneal administration for 3 days. Based on the outcome, we used 25 mg/kg NP-14 and 50 mg/kg HND-007 for further experiments. For NP-10, further dose escalation above 100 mg/kg could not be achieved because of its insolubility; therefore, we used this dose for subsequent experiments.

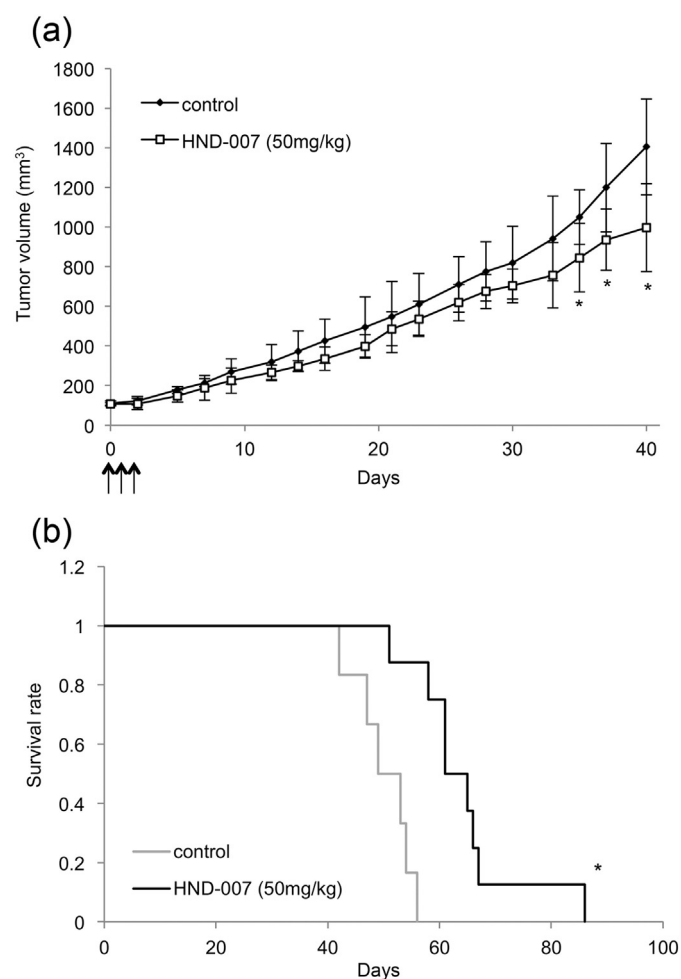


Fig. 6. HND-007 suppresses growth of HeLa tumors in nude mice. (a) HeLa cells were subcutaneously inoculated into BALB/c-nu nude mice. The mice were treated with 50 mg/kg of HND-007 or control vehicle ($n = 8$, $n = 6$ respectively), as described in Materials and methods. The mean tumor volumes (with SDs) are shown. Arrows represent the days of drug administration. *, $p < 0.05$ (compared with vehicle). (b) Kaplan–Meier curves obtained in the experiments shown above. *, $p < 0.05$ (compared with vehicle; Kaplan–Meier estimate).

Nude mice bearing HeLa cell tumors were treated with control vehicle or one of the three compounds at the doses described above, once daily for 3 days (intra-peritoneal injection). For NP-14 and NP-10, we did not observe a significant anti-tumor effect (data not shown). On the other hand, HND-007 exhibited a statistically significant anti-tumor effect under these experimental conditions (Fig. 6), although its efficacy for treatment of HeLa cell tumors in nude mice appears lower than that reported for paclitaxel [34,35]. Based on these findings, we concluded that HND-007 is a promising lead compound for development of novel anti-mitotic, anti-microtubule chemotherapeutic agents.

At this time, we have not observed any anti-tumor activity of NP-10. However, this compound may have a novel mitotic target molecule(s), and may achieve cancer cell-specific induction of mitotic arrest. Therefore, it would be useful to perform further experiments aimed at clarifying the target molecule(s) of NP-10 and improving its anti-tumor activity by synthesizing related compounds.

Disclosure statement

The authors declare no conflict of financial interest.

Transparency document

The Transparency document associated with this article can be found, in the online version.

Acknowledgements

We thank Dr. Takeshi Urano for plasmid pcDNA-myc3-Eg5, Dr. Fumiaki Koizumi for PC-14 and PC-14/TXT cells, Dr. Hiroshi Masumoto for anti-CENP-B antibody, Dr. Miho Ohsugi for critical discussion, and Ms. Ryoko Honda for synthesis of some compounds. This work was supported in part by Grants to M.F. from the Ministry of Education, Culture, Sports, Science, and Technology of Japan (AS232Z00220G and 12723068) and the Princess Takamatsu Cancer Research Fund (10-24217). We appreciate the support from the Research Support Center, Graduate School of Medical Sciences, Kyushu University and Center for Clinical and Translational Research of Kyushu University Hospital.

Appendix A. Supplementary data

Supplementary data to this article can be found online at <http://dx.doi.org/10.1016/j.bbagen.2015.04.013>.

References

- [1] K.S. Chan, C.G. Koh, H.Y. Li, Mitosis-targeted anti-cancer therapies: where they stand, *Cell Death Dis.* 3 (2012) (e411).
- [2] M. Kavallaris, Microtubules and resistance to tubulin-binding agents, *Nat. Rev. Cancer* 10 (2010) 194–204.
- [3] M.R. Harrison, K.D. Holen, G. Liu, Beyond taxanes: a review of novel agents that target mitotic tubulin and microtubules, kinases, and kinesins, *Clin. Adv. Hematol. Oncol.* 7 (2009) 54–64.
- [4] M.A. Jordan, L. Wilson, Microtubules as a target for anticancer drugs, *Nat. Rev. Cancer* 4 (2004) 253–265.
- [5] D.A. Brito, C.L. Rieder, The ability to survive mitosis in the presence of microtubule poisons differs significantly between human nontransformed (RPE-1) and cancer (U2OS, HeLa) cells, *Cell Motil. Cytoskeleton* 66 (2009) 437–447.
- [6] K.E. Gascoigne, S.S. Taylor, Cancer cells display profound intra- and interline variation following prolonged exposure to antimetabolic drugs, *Cancer Cell* 14 (2008) 111–122.
- [7] T.J. Mitchison, The proliferation rate paradox in antimetabolic chemotherapy, *Mol. Biol. Cell* 23 (2012) 1–6.
- [8] J.W. Lippert 3rd, Vascular disrupting agents, *Bioorg. Med. Chem.* 15 (2007) 605–615.
- [9] S. De, R. Cipriano, M.W. Jackson, G.R. Stark, Overexpression of kinesins mediates docetaxel resistance in breast cancer cells, *Cancer Res.* 69 (2009) 8035–8042.
- [10] M.C. Henderson, Y.J. Shaw, H. Wang, H. Han, L.H. Hurley, G. Flynn, R.T. Dorr, D.D. Von Hoff, UA62784, a novel inhibitor of centromere protein E kinesin-like protein, *Mol. Cancer Ther.* 8 (2009) 36–44.
- [11] T. Takeuchi, S. Oishi, T. Watanabe, H. Ohno, J. Sawada, K. Matsuno, A. Asai, N. Asada, K. Kitaura, N. Fujii, Structure-activity relationships of carboline and carbazole

- derivatives as a novel class of ATP-competitive kinesin spindle protein inhibitors, *J. Med. Chem.* 54 (2011) 4839–4846.
- [12] S. Oishi, T. Watanabe, J. Sawada, A. Asai, H. Ohno, N. Fujii, Kinesin spindle protein (KSP) inhibitors with 2,3-fused indole scaffolds, *J. Med. Chem.* 53 (2010) 5054–5058.
- [13] K.W. Wood, L. Lad, L. Luo, X. Qian, S.D. Knight, N. Nevins, K. Brejck, D. Sutton, A.G. Gilmartin, P.R. Chua, R. Desai, S.P. Schauer, D.E. McNulty, R.S. Annan, L.D. Belmont, C. Garcia, Y. Lee, M.A. Diamond, L.F. Faucette, M. Giardiniere, S. Zhang, C.M. Sun, J.D. Vidal, S. Lichtsteiner, W.D. Cornwell, J.D. Greshock, R.F. Wooster, J.T. Finan, R.A. Copeland, P.S. Huang, D.J. Morgans Jr., D. Dhanak, G. Bergnes, R. Sakowicz, J.R. Jackson, Antitumor activity of an allosteric inhibitor of centromere-associated protein-E, *Proc. Natl. Acad. Sci. U. S. A.* 107 (2010) 5839–5844.
- [14] D. Huszar, M.E. Theoclitou, J. Skolnik, R. Herbst, Kinesin motor proteins as targets for cancer therapy, *Cancer Metastasis Rev.* 28 (2009) 197–208.
- [15] R. Sakowicz, J.T. Finan, C. Beraud, A. Crompton, E. Lewis, A. Fritsch, Y. Lee, J. Mak, R. Moody, R. Turincio, J.C. Chabala, P. Gonzales, S. Roth, S. Weitman, K.W. Wood, Antitumor activity of a kinesin inhibitor, *Cancer Res.* 64 (2004) 3276–3280.
- [16] S. DeBonis, D.A. Skoufias, L. Lebeau, R. Lopez, G. Robin, R.L. Margolis, R.H. Wade, F. Kozielski, In vitro screening for inhibitors of the human mitotic kinesin Eg5 with antimitotic and antitumor activities, *Mol. Cancer Ther.* 3 (2004) 1079–1090.
- [17] L. Hu, Z.R. Li, Y. Li, J. Qu, Y.H. Ling, J.D. Jiang, D.W. Boykin, Synthesis and structure-activity relationships of carbazole sulfonamides as a novel class of antimitotic agents against solid tumors, *J. Med. Chem.* 49 (2006) 6273–6282.
- [18] A.L. Risinger, C.D. Westbrook, A. Encinas, M. Mulbaier, C.M. Schultes, S. Wawro, J.D. Lewis, B. Janssen, F.J. Giles, S.L. Mooberry, ELR510444, a novel microtubule disruptor with multiple mechanisms of action, *J. Pharmacol. Exp. Ther.* 336 (2011) 652–660.
- [19] J.J. Field, J.F. Diaz, J.H. Miller, The binding sites of microtubule-stabilizing agents, *Chem. Biol.* 20 (2013) 301–315.
- [20] N. Sugimoto, T. Yugawa, M. Iizuka, T. Kiyono, M. Fujita, Chromatin remodeler *snr2* homolog 2 (SNF2H) is recruited onto DNA replication origins through interaction with Cdc10 protein-dependent transcript 1 (Cdt1) and promotes pre-replication complex formation, *J. Biol. Chem.* 286 (2011) 39200–39210.
- [21] D. Liu, M. Vleugel, C.B. Backer, T. Hori, T. Fukagawa, I.M. Cheeseman, M.A. Lampson, Regulated targeting of protein phosphatase 1 to the outer kinetochore by KNL1 opposes Aurora B kinase, *J. Cell Biol.* 188 (2010) 809–820.
- [22] Y. Mizushima, T. Takeuchi, Y. Takakusagi, Y. Yonezawa, T. Mizuno, K. Yanagi, N. Imamoto, F. Sugawara, K. Sakaguchi, H. Yoshida, M. Fujita, Coenzyme Q10 as a potent compound that inhibits Cdt1-geminin interaction, *Biochim. Biophys. Acta* 1780 (2008) 203–213.
- [23] M. Melixetian, A. Ballabeni, L. Masiero, P. Gasparini, R. Zamponi, J. Bartek, J. Lukas, K. Helin, Loss of Geminin induces rereplication in the presence of functional p53, *J. Cell Biol.* 165 (2004) 473–482.
- [24] Y. Hayashi-Takanaka, K. Yamagata, N. Nozaki, H. Kimura, Visualizing histone modifications in living cells: spatiotemporal dynamics of H3 phosphorylation during interphase, *J. Cell Biol.* 187 (2009) 781–790.
- [25] F.J. Oliver, G. de la Rubia, V. Rolli, M.C. Ruiz-Ruiz, G. de Murcia, J.M. Murcia, Importance of poly(ADP-ribose) polymerase and its cleavage in apoptosis. Lesson from an uncleavable mutant, *J. Biol. Chem.* 273 (1998) 33533–33539.
- [26] N. Nishimoto, M. Watanabe, S. Watanabe, N. Sugimoto, T. Yugawa, T. Ikura, O. Koiwai, T. Kiyono, M. Fujita, Heterocomplex formation by Arp4 and beta-actin is involved in the integrity of the Brg1 chromatin remodeling complex, *J. Cell Sci.* 125 (2012) 3870–3882.
- [27] H. Maiato, E. Logarinho, Mitotic spindle multipolarity without centrosome amplification, *Nat. Cell Biol.* 16 (2014) 386–394.
- [28] Y. Funayama, S. Ohta, N. Kubota, K. Nishio, H. Arioka, H. Ogasawara, T. Ohira, F. Kanazawa, S. Hasegawa, N. Saijo, Establishment of a docetaxel-resistant human non-small cell lung cancer cell line, *Cell. Pharmacol.* 2 (1995) 303–309.
- [29] P. Giannakakou, D.L. Sackett, Y.K. Kang, Z. Zhan, J.T. Buters, T. Fojo, M.S. Poruchynsky, Paclitaxel-resistant human ovarian cancer cells have mutant beta-tubulins that exhibit impaired paclitaxel-driven polymerization, *J. Biol. Chem.* 272 (1997) 17118–17125.
- [30] K. Tsujimura, M. Ogawara, Y. Takeuchi, S. Imajoh-Ohmi, M.H. Ha, M. Inagaki, Visualization and function of vimentin phosphorylation by cdc2 kinase during mitosis, *J. Biol. Chem.* 269 (1994) 31097–31106.
- [31] F. Toyoshima-Morimoto, E. Taniguchi, N. Shinya, A. Iwamatsu, E. Nishida, Polo-like kinase 1 phosphorylates cyclin B1 and targets it to the nucleus during prophase, *Nature* 410 (2001) 215–220.
- [32] M. Kwon, S.A. Godinho, N.S. Chandhok, N.J. Ganem, A. Azioune, M. Thery, D. Pellman, Mechanisms to suppress multipolar divisions in cancer cells with extra centrosomes, *Genes Dev.* 22 (2008) 2189–2203.
- [33] B. Leber, B. Maier, F. Fuchs, J. Chi, P. Riffel, S. Anderhub, L. Wagner, A.D. Ho, J.L. Salisbury, M. Boutros, A. Kramer, Proteins required for centrosome clustering in cancer cells, *Sci. Transl. Med.* 2 (2010) (33ra38).
- [34] K.S. Chung, H.E. Choi, J.S. Shin, Y.W. Cho, J.H. Choi, W.J. Cho, K.T. Lee, 6,7-Dimethoxy-3-(3-methoxyphenyl)isoquinolin-1-amine induces mitotic arrest and apoptotic cell death through the activation of spindle assembly checkpoint in human cervical cancer cells, *Carcinogenesis* 34 (2013) 1852–1860.
- [35] M. Jemaa, L. Galluzzi, O. Kepp, L. Senovilla, M. Brands, U. Boemer, M. Koppitz, P. Lienau, S. Precht, V. Schulze, G. Siemeister, A.M. Wengner, D. Mumberg, K. Ziegelbauer, A. Abrieu, M. Castedo, I. Vitale, G. Kroemer, Characterization of novel MPS1 inhibitors with preclinical anticancer activity, *Cell Death Differ.* 20 (2013) 1532–1545.